

pubs.acs.org/NanoLett Letter

# Controlling Phase Conversion of Cu-Sb-Se Nanoparticles through the Use of an Amide Base

Amanda R. Kale, William E. Bullett, and Amy L. Prieto\*



Cite This: Nano Lett. 2023, 23, 5460-5466



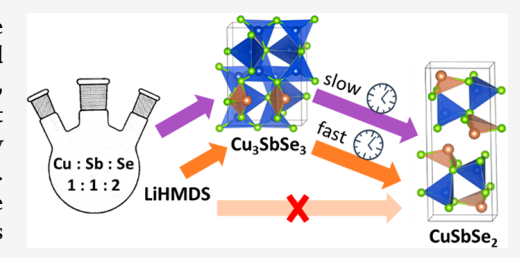
**ACCESS** I

III Metrics & More

Article Recommendations

Supporting Information

**ABSTRACT:** The family of copper antimony selenides is important for renewable energy applications. Several phases are accessible within narrow energy and compositional ranges, and tunability between phases is not well-established. Thus, this system provides a rich landscape to understand the phase transformations that occur in hot-injection nanoparticle syntheses. Rietveld refinements on X-ray diffraction patterns model anisotropic morphologies to obtain phase percentages. Reactions targeting the stoichiometry of CuSbSe<sub>2</sub> formed Cu<sub>3</sub>SbSe<sub>3</sub> before decomposing to thermodynamically stable CuSbSe<sub>2</sub> over time. An amide base was added to balance cation reactivity and directly form CuSbSe<sub>2</sub>. Interestingly,



 $Cu_3SbSe_3$  remained present but converted to  $CuSbSe_2$  more rapidly. We propose that initial  $Cu_3SbSe_3$  formation may be due to the selenium species not being reactive enough to balance the high reactivity of the copper complex. The unexpected effect of a base on cation reactivity in this system provides insight into the advantages and limitations for its use in other multivalent systems.

**KEYWORDS:** copper antimony selenide, precursor reactivity, amide, amide-assisted, amide-promoted, LiHMDS, reaction pathway, nanoparticles, anisotropic, Rietveld refinement

opper antimony chalcogenides are of interest for photovoltaics<sup>1,2</sup> and thermoelectrics<sup>3,4</sup> due to their attractive optoelectronic properties and because they are composed of less toxic, more abundant elements. In the Cu-Sb-Se system, three ternary phases exist (CuSbSe<sub>2</sub>, Cu<sub>3</sub>SbSe<sub>3</sub>, Cu<sub>3</sub>SbSe<sub>4</sub>) that have been shown to have similar stabilities in solution, making phase impurities a challenge in some syntheses.<sup>5–7</sup> While all three ternary nanoparticle phases have been synthesized in isolation, <sup>5,8,9</sup> an understanding of the synthetic parameters that favor each ternary phase has not been demonstrated. Thus, the Cu-Sb-Se system is rich for the exploration of the effect of precursor reactivity on phase formation.

A common problem in multinary copper chalcogen syntheses is that one cationic precursor is often more reactive than the other, resulting in the formation of binary phases as "sinks" or solid solutions rich in one cation. One method of controling precursor reactivity in these systems is through the addition of a reagent that favors the formation of more reactive cation complexes. The base lithium bis(trimethylsilylamide) (LiHMDS) has been used to form reactive complexes in syntheses with trioctylphosphine (TOP), the metal silylamide intermediates form. LiHMDS has also been used in syntheses with oleylamine (OLA), the acting as a Brønsted base and deprotonating the oleylamine to form reactive oleylamide complexes in solution.

While the understanding of precursor reactivity in nanoparticle synthesis has greatly increased in recent years, the development of unifying trends that can be used to design syntheses of new and unexplored systems remains a challenge in the field. If we can collectively define precursor reactivity with respect to the relative rate of atom incorporation into the final product, then synthetic methods using similar precursors could be more readily applied to new materials. Here we define precursor reactivity in relation to the stability of the active complex that forms just prior to injection. A less stable active complex with easily dissociating leaving groups will be more likely to decompose and have its atom incorporate into a crystal structure, and we would call this precursor more reactive.

In this work, we aim to explore phase control in the Cu-Sb-Se system through the control of precursor reactivity. We show that metastable Cu<sub>3</sub>SbSe<sub>3</sub> particles generally formed first, which then decomposed into thermodynamically stable CuSbSe<sub>2</sub> sheets in reactions with oleylamine. We then attempted to alter precursor reactivity through the addition of LiHMDS in order to bypass the formation of the metastable phase and directly nucleate CuSbSe<sub>2</sub>. In doing so, we test the applicability of LiHMDS to control reactivity in unexplored chalcogenide systems.

In the standard synthesis, CuCl<sub>2</sub> (0.5 mmol), SbCl<sub>3</sub> (0.5 mmol), and oleylamine (4 or 7 mL, OLA) were combined air-

Received: February 8, 2023 Revised: May 23, 2023 Published: June 13, 2023





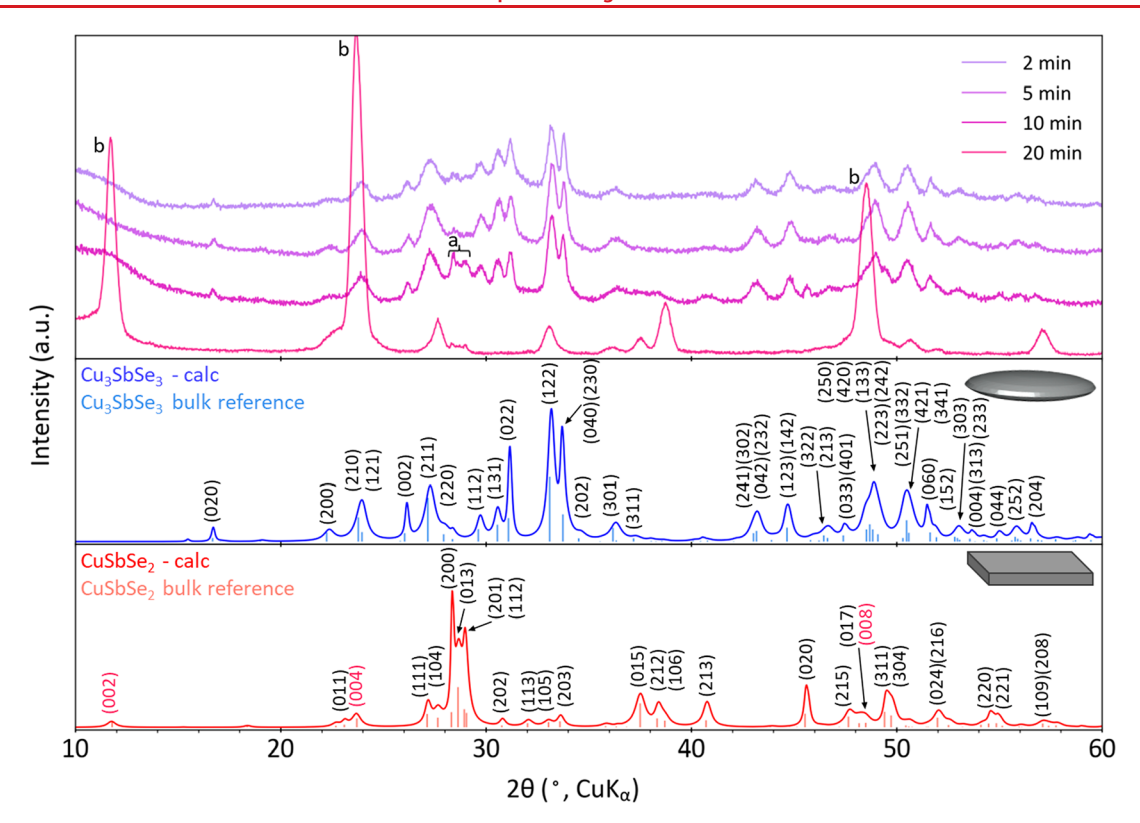


Figure 1. Powder X-ray diffraction patterns of 7 mL OLA syntheses. Calculated patterns of Cu<sub>3</sub>SbSe<sub>3</sub> and CuSbSe<sub>2</sub> sheets of the approximate dimensions in PXRD patterns are superimposed onto the bulk reference patterns.

free in a flask and held at 90  $^{\circ}$ C for 30 min under  $N_2$ . In reactions with LiHMDS, 1 mmol was added to the flask containing the metal salts. The standard Se precursor was prepared by dissolving Se (1 mmol), in an alkahest solution of oleylamine and dodecanethiol. The flask was heated to 150 °C, and the contents changed in color from blue to orange while heating. This color change has been observed in other Cu systems and is commonly cited as the conversion from  $Cu^{2+}$  to  $Cu^{+}$  <sup>19</sup> Upon reaching 150 °C, the room-temperature Se precursor was injected, and particles were quenched into test tubes after the desired growth times. Powder X-ray diffraction (PXRD) patterns and subsequent Rietveld refinements were used to assess the nanocrystalline phases present and their relative quantities. Anisotropic particle morphologies were modeled for each phase using the method of Ectors et al. (additional details are given in the Supporting Information).<sup>20</sup> Transmission and scanning electron microscopy (TEM, SEM) were used to image nanoparticles and assess morphology.

To determine how the phase transformation pathway of Cu-Sb-Se ternary phases proceeded, we performed PXRD on the reaction products as time progressed. Despite a starting precursor ratio of 1:1:2 Cu:Sb:Se, PXRD patterns show that primarily crystalline  $\text{Cu}_3\text{SbSe}_3$  is present at 2 min (Figure 1). The peaks denoted by a are  $\text{CuSbSe}_2$ , which increase in intensity over time as  $\text{Cu}_3\text{SbSe}_3$  peaks corresponding to  $\text{Cu}_3\text{SbSe}_3$  disappear. At 20 min,  $\text{CuSbSe}_2$  dominates, with substantial preferential orientation observed in the  $\{001\}$  planes, b, due to nanosheet stacking.

TEM images and fast-Fourier transforms (FFTs) of lattice planes show particles with a variety of crystalline phases and morphologies (Figure 2 and Figure S1). At short times, 2 and 5 min, mostly small Cu<sub>3</sub>SbSe<sub>3</sub> platelets are observed, along with small particles of low crystallinity (Figure 2A–H). In the 10

min aliquot, long, polycrystalline CuSbSe<sub>2</sub> ribbons are observed. As the reaction progresses to 20 min, larger, crystalline CuSbSe<sub>2</sub> sheets are observed that may have been formed from the coalescence of ribbons observed in the 10 min aliquot.

The anisotropic morphologies observed in TEM are consistent with patterns of anisotropic broadening observed in and modeled from PXRD patterns. This correlation is illustrated in Figure 3. CuSbSe $_2$  sheet growth is limited in [001], which has been attributed to van der Waals gaps between the layers, caused by the Sb lone pairs.  $^4$  Cu $_3$ SbSe $_3$  platelet growth is limited in [100], which is also consistent with growth inhibited by Sb lone pairs. It is possible that oleylamine binds strongly to these Sb sites, further discouraging growth.

We hypothesized that Cu-rich Cu<sub>3</sub>SbSe<sub>3</sub> initially formed due to the active copper complex being more reactive than the active antimony complex. This difference in reactivity between cations has been explained with hard—soft acid—base theory. As Sb<sup>3+</sup> is a harder acid than Cu<sup>+</sup> and oleylamine and chloride are hard bases, it is expected that a hard—hard interaction of Sb<sup>3+</sup> will lead to stronger bonds with available ligands, making its active coordination complex less likely to decompose to incorporate into a crystal structure. However, Cu<sup>+</sup>, as a soft acid, is expected to form weaker bonds with the available ligands, making its complex less stable and more likely to incorporate into a crystal structure, favoring a Cu-rich phase.

The degradation of  $Cu_3SbSe_3$  to  $CuSbSe_2$  over time is supported by thermodynamic values. Of the three ternary phases,  $CuSbSe_2$  has the most negative calculated  $H_f$  value, -0.249 eV/atom, while  $Cu_3SbSe_3$  has the most positive  $H_f$  value, -0.175 eV/atom, and is the only ternary predicted to be unstable at its composition. We propose that  $Cu_3SbSe_3$  is a

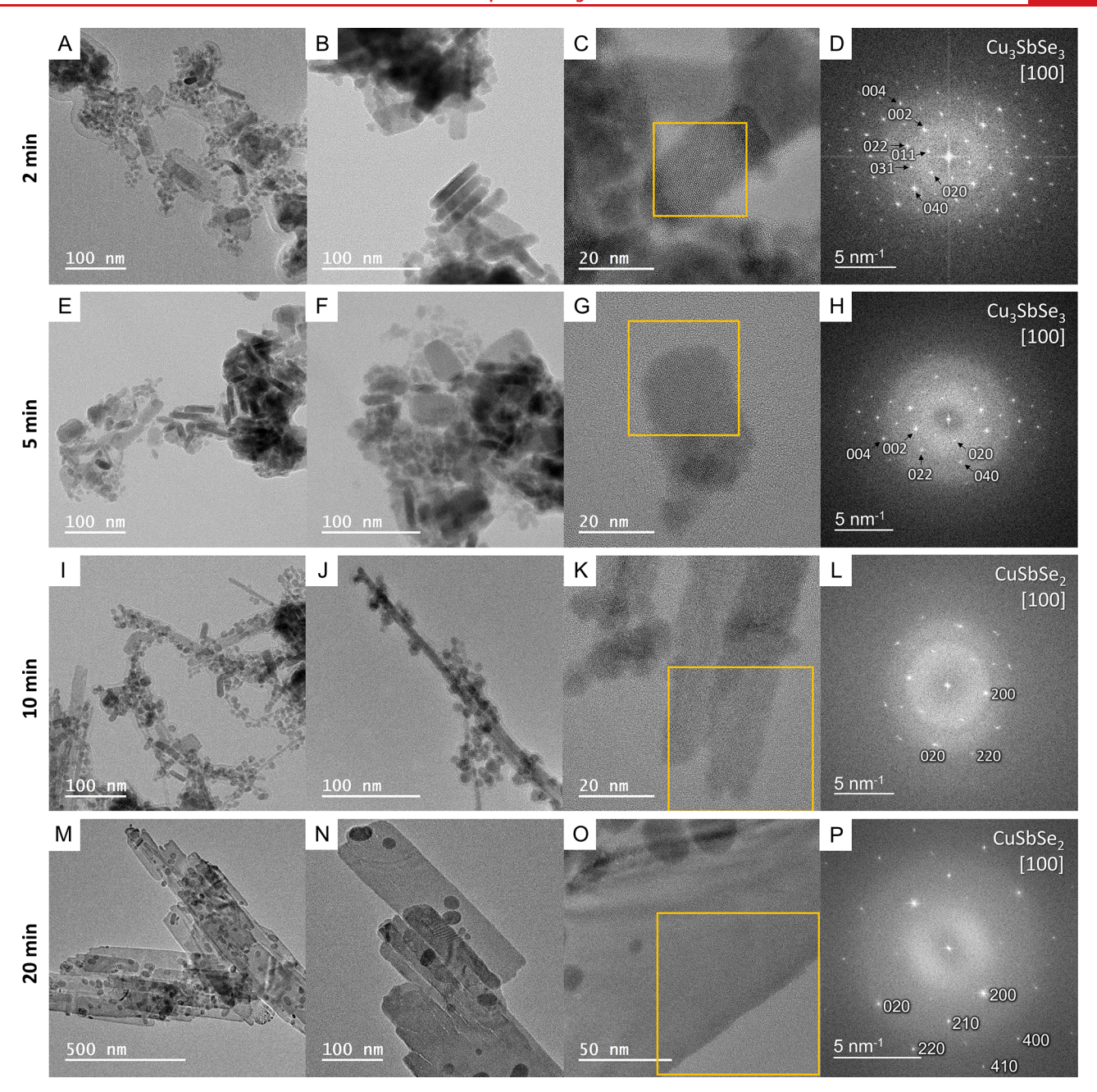


Figure 2. TEM images of the 7 mL OLA syntheses of 2 min (A-C), 5 min (E-G), 10 min (I-L) and 20 min (M-P) aliquots. (D), (H), (L), and (P) are FFTs of the image on the left.

metastable phase that decomposes to the thermodynamically stable CuSbSe<sub>2</sub>. To further test the metastable behavior, Cu<sub>3</sub>SbSe<sub>3</sub> particles were isolated using an established phase-pure synthesis under similar solution conditions<sup>24</sup> and were heated in oleylamine or squalane. PXRD patterns of these products show that Cu<sub>3</sub>SbSe<sub>4</sub> forms instead of the predicted CuSbSe<sub>2</sub> (Figure S2). The formation of Cu<sub>3</sub>SbSe<sub>4</sub> impurities from Cu<sub>3</sub>SbSe<sub>3</sub> particles has been observed in the literature, further supporting that the conversion landscape of Cu<sub>3</sub>SbSe<sub>3</sub> particles is highly dependent on solution conditions. In particular, it appears that Cu and Sb species are required for CuSbSe<sub>2</sub> formation, as shown in eq 1. As many possible active complexes exist, those listed here are simply potential species. While it is possible that conversion could occur through Sb and Se diffusion into Cu<sub>3</sub>SbSe<sub>3</sub>, we do not see evidence of this

in XRD or TEM and propose that Cu<sub>3</sub>SbSe<sub>3</sub> decomposes back into Cu and Sb species prior to CuSbSe<sub>2</sub> formation.

$$Cu_3SbSe_3 + 2SbCl_3(RNH_2)_{3-x} + 3Se_8^{2-}(RNH_3^+)_y$$
  
 $\rightarrow 3CuSbSe_2 + oleylamine + byproducts$  (1)

One question that remains is why does Cu<sub>3</sub>SbSe<sub>3</sub> form initially under these conditions instead of Cu<sub>3</sub>SbSe<sub>4</sub>, given that both are copper-rich phases? The compound Cu<sub>3</sub>SbSe<sub>3</sub> is Sedeficient compared to Cu<sub>3</sub>SbSe<sub>4</sub>, so its formation could be encouraged by slower incorporation of selenium. We performed the synthesis with a Cu:Sb:Se ratio of 3:1:4 to test whether Cu<sub>3</sub>SbSe<sub>3</sub> would still form. Mostly Cu<sub>3</sub>SbSe<sub>4</sub> is formed, though some Cu<sub>3</sub>SbSe<sub>3</sub> is present at 5 min (Figure S3). We propose that some Cu<sub>3</sub>SbSe<sub>3</sub> formed initially with

Nano Letters pubs.acs.org/NanoLett Letter

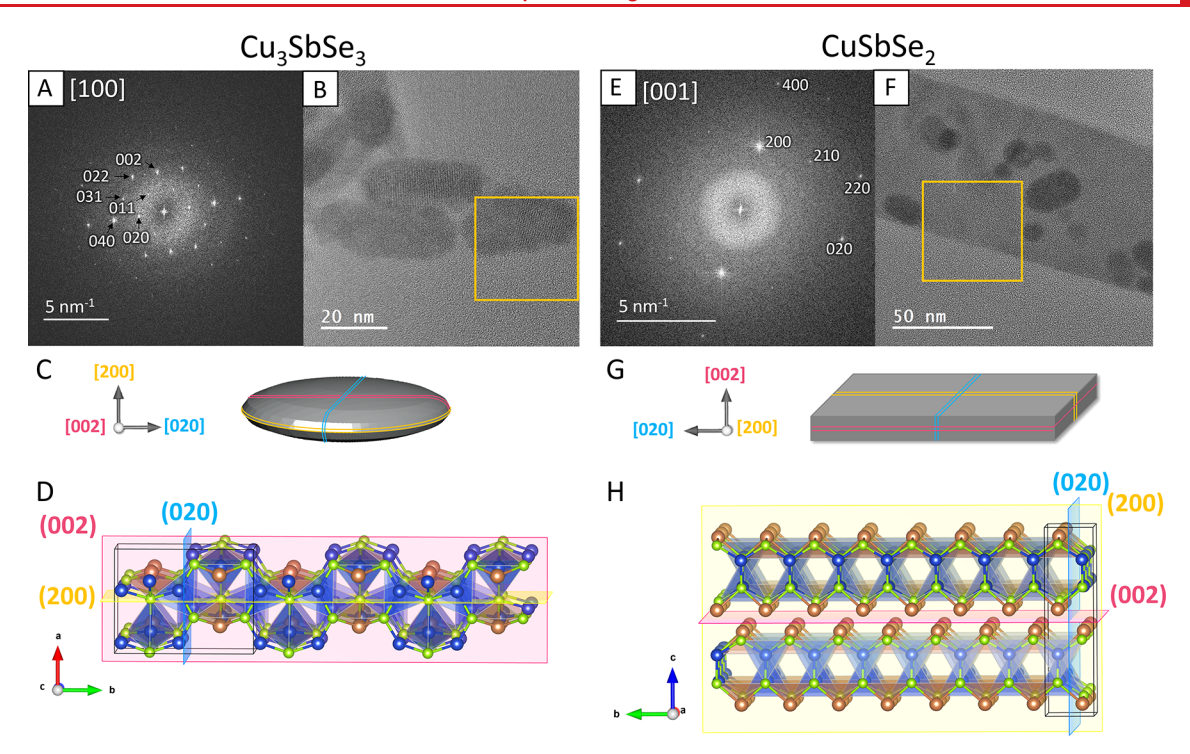


Figure 3. Structural characterization comparison of  $CuSbSe_2$  (A–D) and  $Cu_3SbSe_3$  (E, F). FFT and corresponding image of (A, B)  $Cu_3SbSe_3$  and (E, F)  $CuSbSe_2$ . Anisotropic growth model showing the aspect ratio obtained from PXRD patterns for  $Cu_3SbSe_3$  (C) and  $CuSbSe_2$  (G). Crystal structure corresponding to anisotropic growth for (D)  $Cu_3SbSe_3$  and (H)  $CuSbSe_2$ .

both 1:1:2 and 3:1:4 ratios of Cu:Sb:Se because the room-temperature Se precursor is not as reactive as the 150  $^{\circ}$ C cation complexes.

With the goal of bypassing the Cu<sub>3</sub>SbSe<sub>3</sub> intermediate phase and directly nucleating the Cu<sub>5</sub>SbSe<sub>2</sub> phase that matches the starting stoichiometry, we used a silylamide-promoted approach, which has been successful with other ternary Cu and Sb chalcogenide systems. <sup>13,15</sup> We aimed to test whether the addition of a silylamide base could be used to increase the reactivity of the harder acid Sb<sup>3+</sup> in this system. We hypothesized that increasing the reactivity of the Sb complex would encourage Cu and Sb incorporation at similar rates and would allow us to directly nucleate Cu<sub>5</sub>SbSe<sub>2</sub>.

Rietveld refinements were performed on XRD patterns to estimate the percent of crystalline phases in aliquots at each time from reactions with and without base (Figure 4, Figures S4-S6, and Table S1). In most reactions, a majority of Cu<sub>3</sub>SbSe<sub>3</sub> platelets are observed initially, which converted to larger CuSbSe2 sheets over time. In the 4 mL OLA, 4 mL injection synthesis (Figure S7), almost entirely Cu<sub>3</sub>SbSe<sub>3</sub> is formed initially both with and without base. The formation of mostly Cu<sub>3</sub>SbSe<sub>3</sub> at short times when base is present disproves our initial hypothesis that the base would cause direct nucleation of CuSbSe<sub>2</sub>. However, the addition of base does cause faster conversion from Cu<sub>3</sub>SbSe<sub>3</sub> to CuSbSe<sub>2</sub>. This is exaggerated in reactions with smaller volumes of OLA, which is likely due to the higher concentration of base (Figure S6). This is also apparent in SEM images, as a greater proportion of large CuSbSe<sub>2</sub> sheets are present in the 5 min LiHMDS sample than the sample without base (Figure S8).

In previous work, our group characterized solutions of oleylamine with varying concentrations of LiHMDS and showed that substantial oleylamide formation is observed when the ratio of amine to LiHMDS is 14:1. In the reaction

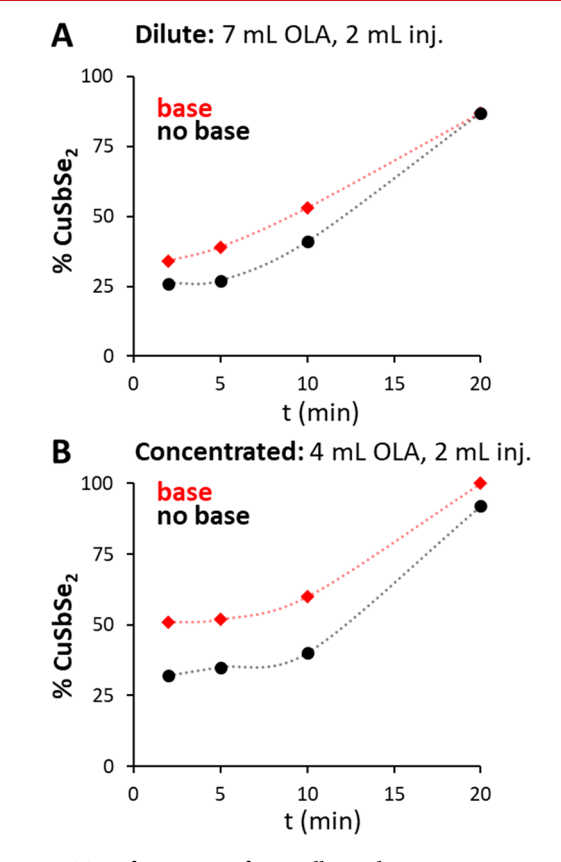


**Figure 4.** Transformation of crystalline phases present over time under various reaction conditions. Rietveld refinements were used to estimate mol percentages (Figures S4—S6). Note that dotted lines are included to guide the reader's eye and do not represent fits of the data.

with 4 mL of OLA, the ratio is  $\sim$ 12:1, and we propose that the higher ratio in the 4 mL reaction causes a greater formation of oleylamide species, increasing the reactivity of the cations more than in the 7 mL synthesis. Although this ratio would decrease upon addition of the Se precursor, other work has shown that when a metal is present, the equilibrium between OLA and oleylamide is often pushed toward the amide products, 16 and thus we propose that the formation of oleylamide species would be greater in the 4 mL synthesis. Additionally, the higher concentration of cations in the flask may make it more favorable for the unstable oleylamides to complex to the metal ions. We propose that the faster conversion to the CuSbSe<sub>2</sub> phase over time in the presence of base may be due to the decomposition of Sb-amide in solution after Cu<sub>3</sub>SbSe<sub>3</sub> has already formed. Future characterization of these species would help to further elucidate reaction pathway.

Reactions were also performed with *n*-butylithium (*n*-BuLi), anticipating that the stronger base would produce higher concentrations of metal amide complexes, in turn encouraging more rapid formation of CuSbSe<sub>2</sub>. Instead, a similar proportion of CuSbSe<sub>2</sub> was observed as when LiHMDS was added for the 7 mL reaction (Figure S9). We propose that a similar concentration of amide species must be present to obtain a similar proportion of Cu-rich and Cu-poor phases. Alternatively, it is possible that a lower concentration of Se available for incorporation may necessitate the initial formation of Cu<sub>3</sub>SbSe<sub>3</sub>. Only after the Se precursor is fully heated to reaction temperature will the effects of the added base be observed, resulting in an increase in the rate of conversion to the CuSbSe<sub>2</sub> phase.

The initial formation of Cu<sub>3</sub>SbSe<sub>3</sub>, even in the presence of base that should lead to the formation of more reactive species, suggests that the copper complex remains too reactive for Cu<sup>+</sup> and Sb<sup>3+</sup> to incorporate at similar rates. This is slightly surprising given that amide-promoted syntheses have been successful with Cu in the literature. In a silylamide synthesis of Cu-In-Se nanoparticles, Yarema et al. were able to synthesize CuInSe<sub>2</sub> nanoparticles with the chloride salts in both OLA and TOP.<sup>25</sup> In more recent work, without the use of silylamide, Yarema et al. were able to synthesize CuSbSe2 nanoparticles under conditions very similar to ours with the use of CuCl and obtained phase purity at temperatures above 120 °C.8 One important distinction in both systems may be the use of CuCl instead of CuCl<sub>2</sub>, as the reduction of Cu<sup>2+</sup> to Cu<sup>+</sup> in our system may change the coordinating ligand, altering precursor reactivity. However, we synthesized particles with CuCl, instead of CuCl2, under our reaction conditions, and the resulting products are nearly identical to those obtained with Cu<sup>2+</sup> (Figure S10). Another key difference may be the preparation method of the Se precursor, as Yarema et al. prepared their Se precursor as a stock solution, which may result in a difference in Se solvation compared to ours.

This supports our hypothesis that the Se precursor may play a role in favoring the initial formation of Cu<sub>3</sub>SbSe<sub>3</sub>, as this phase is Se-deficient compared to the other ternary phases. Some inconsistencies between reactions products observed when Se precursors were prepared with different sonicators and/or stir times caused us to question whether changes in the solvation of the Se precursor affects phase formation. To test this hypothesis, separate reactions were performed with stirring of the Se precursor for 15 and 40 min. The reaction with a longer Se precursor stir time gave considerably more CuSbSe<sub>2</sub> at 5 min (Figure S11). Assuming that a longer stir time leads to

greater dissolution of the Se precursor, we propose that the increased formation of CuSbSe<sub>2</sub> is due to an increased concentration of Se available for incorporation. It is possible that with an even better solvated Se precursor, the Cu<sub>3</sub>SbSe<sub>3</sub> phase may be bypassed entirely, which would be consistent with its lack of observation by Yarema et al. Due to the dissolution of the Se precursor altering the rate of phase transformation, we kept its preparation consistent to measure the impact of the cations in solution.

The purpose of using amide-promoted syntheses is to make reactive complexes of both cations, making differences in hard-soft pairings obsolete. If the base is not used in high enough excess, this will not be the case, and the effects of the complexation with the original solvent will still be evident. Yarema et al. observed this in the synthesis of Ag-In-Se NPs: high concentrations of amide were required to observe incorporation of In and Ag in the final product that corresponded to the initial ratios of In and Ag added. 12 This could explain why in our case it appears that the hard-soft acid—base mismatch for the Cu<sup>+</sup> complex may remain an issue. However, in our system, reactions using a higher amount of amide (3 mmol) appeared to result in the formation of Cu in the reaction flask, identified by its characteristic red color, and only Cu<sub>3</sub>SbSe<sub>3</sub> was observed in PXRD (Figure S12). As the active Cu precursor was likely changed in these reactions, only smaller quantities of LiHMDS were used.

Another important distinction between literature syntheses that use LiHMDS and that herein is that amide bases are typically included in the injection solution, while ours is added to the reaction flask. Adding LiHMDS to the previously used Se alkahest solution inhibited the dissolution of both solids. The replacement of the alkahest Se solution with a TOPSe precursor, commonly used with LiHMDS, resulted in the formation of only Sb<sup>0</sup> (Figure S13). We opted to then add the base to the reaction flask, which maintained the solubility of the Se precursor. An alternative approach that preserves the integrity of the Se precursor is to inject both Se and amide base separately. While a number of double-injection reactions were performed, separating the bases into different mediums, the results appeared similar to reactions without base, likely due to the fact that the room-temperature base solutions took additional time to form metal oleylamide complexes when compared to the standard base reactions (Figure S14).

Additional double-injection reactions were performed by separating Sb and LiHMDS into a flask in OLA, with the goal of preforming Sb oleylamide complexes, and once dissolved, this solution and the Se precursor were injected into a flask containing CuCl<sub>2</sub> and OLA (Figure S15). The most Sbdeficient phase, Cu<sub>3</sub>SbSe<sub>4</sub>, was favored, with slightly more CuSbSe<sub>2</sub> present when base was added. The Sb species may have been even less reactive because the injected solution was at room temperature, directing initial phase formation to the most Sb-deficient. In a synthesis with the Sb-LiHMDS flask heated to the reaction temperature prior to injection, Cu<sub>3</sub>SbSe<sub>3</sub> is observed again instead of Cu<sub>3</sub>SbSe<sub>4</sub>, and more CuSbSe<sub>2</sub> is present in the reaction flask than with the room-temperature injection (Figure S16). This may point to, once again, Se being the directing factor for initial Cu<sub>3</sub>SbSe<sub>3</sub> formation. In-depth studies with the Se precursor would need to be performed to determine if this is the case and is thus beyond the scope of this work.

In this work we have begun to decouple the variable rates of reactivity of the cations and anions, thereby developing a better Nano Letters pubs.acs.org/NanoLett Letter

understanding of phase control in the Cu-Sb-Se system. Under our reaction conditions, metastable Cu<sub>3</sub>SbSe<sub>3</sub> forms initially and decomposes to CuSbSe2 over time. However, without any Sb or Se complexes in solution, Cu<sub>3</sub>SbSe<sub>3</sub> decomposes to Cu<sub>3</sub>SbSe<sub>4</sub>, suggesting that monomers in solution are essential to CuSbSe<sub>2</sub> formation. We initially hypothesized that the addition of an amide base would encourage more rapid incorporation of Sb<sup>3+</sup>, resulting in the direct nucleation of CuSbSe<sub>2</sub>. However, mostly Cu<sub>3</sub>SbSe<sub>3</sub> was still observed at short times. It does appear that degradation occurs more quickly with the addition of the silylamide. We hypothesize that this is due to the increased reactivity of the Sb monomer allowing faster formation of CuSbSe2 after Cu3SbSe3 begins to decompose. Formation of the Sb amide may take longer than the formation of the Cu amide. Separate double injections of base or Sb precursor and base were performed in an attempt to decouple variables, but even with heating, CuSbSe<sub>2</sub> could not be formed as the initial phase. It is possible that the selenium precursor is the variable that drives the initial formation of Cu<sub>3</sub>SbSe<sub>3</sub>. Understanding phase control in the Cu-Sb-Se system can be extrapolated to other multinary chalcogenide systems in which one cation tends to incorporate much faster than the other.

#### ASSOCIATED CONTENT

## Supporting Information

The Supporting Information is available free of charge at https://pubs.acs.org/doi/10.1021/acs.nanolett.3c00506.

Additional data and analysis, including PXRD patterns, Rietveld refinements, and electron microscopy (PDF)

#### AUTHOR INFORMATION

# **Corresponding Author**

Amy L. Prieto — Department of Chemistry, Colorado State University, Fort Collins, Colorado 80523, United States; orcid.org/0000-0001-9235-185X; Email: amy.prieto@colostate.edu

#### **Authors**

Amanda R. Kale — Department of Chemistry, Colorado State University, Fort Collins, Colorado 80523, United States; orcid.org/0000-0003-2058-902X

William E. Bullett – Department of Chemistry, Colorado State University, Fort Collins, Colorado 80523, United States

Complete contact information is available at: https://pubs.acs.org/10.1021/acs.nanolett.3c00506

#### **Author Contributions**

A.R.K. designed and performed syntheses, characterization, and manuscript preparation. W.E.B. assisted with designing and performing syntheses, PXRD characterization, and manuscript revisions. A.L.P. assisted with project administration and manuscript editing. All authors have given approval to the final version of the manuscript.

#### **Funding**

This work was supported by NSF Chemistry Macromolecular, Supramolecular, and Nanochemistry program (MSN #2109141).

#### Notes

The authors declare no competing financial interest.

#### ACKNOWLEDGMENTS

The authors wish to thank the Analytical Resources Core (RRID: SCR\_021758) at Colorado State University for instrument access, training, and assistance with sample analysis, especially Roy Geiss, for assistance with TEM.

### ABBREVIATIONS

LiHMDS lithium bis(trimethylsilyl)amide

n-BuLi n-butyllihtiumOLA oleylamineDDT dodecanethiol

PXRD powder X-ray diffraction

TEM transmission electron microscopy SEM scanning electron microscopy

## REFERENCES

- (1) Peccerillo, E.; Durose, K. Copper—Antimony and Copper—Bismuth Chalcogenides—Research Opportunities and Review for Solar Photovoltaics. MRS Energy Sustain 2018, 5 (1), 1–59.
- (2) De Souza Lucas, F. W.; Zakutayev, A. Research Update: Emerging Chalcostibite Absorbers for Thin-Film Solar Cells. *APL Mater.* **2018**, *6* (8), 084501.
- (3) Xie, D.; Zhang, B.; Zhang, A.; Chen, Y.; Yan, Y.; Yang, H.; Wang, G.; Wang, G.; Han, X.; Han, G.; Lu, X.; Zhou, X. High Thermoelectric Performance of Cu<sub>3</sub>SbSe<sub>4</sub> Nanocrystals with Cu<sub>2-x</sub>Se in Situ Inclusions Synthesized by a Microwave-Assisted Solvothermal Method. *Nanoscale* **2018**, *10* (30), 14546–14553.
- (4) Luo, Y.; Du, C.; Liang, Q.; Zheng, Y.; Zhu, B.; Hu, H.; Khor, K. A.; Xu, J.; Yan, Q.; Kanatzidis, M. G. Enhancement of Thermoelectric Performance in CuSbSe<sub>2</sub> Nanoplate-Based Pellets by Texture Engineering and Carrier Concentration Optimization. *Small* **2018**, 14 (50), 1803092.
- (5) Liu, Y.; Yang, J.; Gu, E.; Cao, T.; Su, Z.; Jiang, L.; Yan, C.; Hao, X.; Liu, F.; Liu, Y. Colloidal Synthesis and Characterisation of Cu<sub>3</sub>SbSe<sub>3</sub> Nanocrystals. *J. Mater. Chem. A* **2014**, 2 (18), 6363–6367.
- (6) Hsiang, H. I.; Yang, C. T.; Tu, J. H. Characterization of CuSbSe<sub>2</sub> Crystallites Synthesized Using a Hot Injection Method. *RSC Adv.* **2016**, 6 (101), 99297–99305.
- (7) Agocs, D. B.; Danna, T.; Prieto, A. L. Ambient Surface Stability of Thin Film Nanocrystalline Cu<sub>3</sub>SbSe<sub>4</sub> and Structure-Property Relationships. *ACS Appl. Energy Mater.* **2019**, 2 (3), 1903–1910.
- (8) Yarema, O.; Yarema, M.; Moser, A.; Enger, O.; Wood, V. Composition- And Size-Controlled I-V-VI Semiconductor Nanocrystals. *Chem. Mater.* **2020**, *32* (5), 2078–2085.
- (9) Li, D.; Li, R.; Qin, X. Y.; Song, C. J.; Xin, H. X.; Wang, L.; Zhang, J.; Guo, G. L.; Zou, T. H.; Liu, Y. F.; Zhu, X. G. Co-Precipitation Synthesis of Nanostructured Cu<sub>3</sub>SbSe<sub>4</sub> and Its Sn-Doped Sample with High Thermoelectric Performance. *J. Chem. Soc. Dalt. Trans.* **2014**, *43* (4), 1888–1896.
- (10) Yarema, O.; Yarema, M.; Wood, V. Tuning the Composition of Multicomponent Semiconductor Nanocrystals: The Case of I–III–VI Materials. *Chem. Mater.* **2018**, *30* (5), 1446–1461.
- (11) Yarema, O.; Bozyigit, D.; Rousseau, I.; Nowack, L.; Yarema, M.; Heiss, W.; Wood, V. Highly Luminescent, Size- and Shape-Tunable Copper Indium Selenide Based Colloidal Nanocrystals. *Chem. Mater.* **2013**, 25 (18), 3753–3757.
- (12) Yarema, O.; Yarema, M.; Bozyigit, D.; Lin, W. M. M. M.; Wood, V. Independent Composition and Size Control for Highly Luminescent Indium-Rich Silver Indium Selenide Nanocrystals. *ACS Nano* **2015**, *9* (11), 11134–11142.
- (13) Yarema, O.; Yarema, M.; Lin, W. M. M.; Wood, V. Cu-In-Te and Ag-In-Te Colloidal Nanocrystals with Tunable Composition and Size. *Chem. Commun.* **2016**, *52* (72), 10878–10881.
- (14) Miller, R. C.; Neilson, J. R.; Prieto, A. L. Amide-Assisted Synthesis of Iron Germanium Sulfide (Fe<sub>2</sub>GeS<sub>4</sub>) Nanostars: The Effect of LiN(SiMe<sub>3</sub>)<sub>2</sub> on Precursor Reactivity for Favoring

- Nanoparticle Nucleation or Growth. J. Am. Chem. Soc. 2020, 142 (15), 7023-7035.
- (15) Moser, A.; Yarema, O.; Yarema, M.; Wood, V. Synthesis of Small Ag-Sb-Te Nanocrystals with Composition Control. *J. Mater. Chem. C* **2020**, 8 (45), 15985–15989.
- (16) He, M.; Protesescu, L.; Caputo, R.; Krumeich, F.; Kovalenko, M. V. A General Synthesis Strategy for Monodisperse Metallic and Metalloid Nanoparticles (In, Ga, Bi, Sb, Zn, Cu, Sn, and Their Alloys) via in Situ Formed Metal Long-Chain Amides. *Chem. Mater.* **2015**, 27 (2), 635–647.
- (17) Yarema, M.; Caputo, R.; Kovalenko, M. V. Precision Synthesis of Colloidal Inorganic Nanocrystals Using Metal and Metalloid Amides. *Nanoscale* **2013**, *5* (18), 8398–8410.
- (18) Liu, Y.; Yao, D.; Shen, L.; Zhang, H.; Zhang, X.; Yang, B. Alkylthiol-Enabled Se Powder Dissolution in Oleylamine at Room Temperature for the Phosphine-Free Synthesis of Copper-Based Quaternary Selenide Nanocrystals. *J. Am. Chem. Soc.* **2012**, *134* (17), 7207–7210.
- (19) Parvizian, M.; Duràn Balsa, A.; Pokratath, R.; Kalha, C.; Lee, S.; Van den Eynden, D.; Ibáñez, M.; Regoutz, A.; De Roo, J. The Chemistry of Cu3N and Cu3PdN Nanocrystals\*\*. *Angew. Chemie Int. Ed.* **2022**, *61*, No. e202207013.
- (20) Ectors, D.; Goetz-Neunhoeffer, F.; Neubauer, J. A Generalized Geometric Approach to Anisotropic Peak Broadening Due to Domain Morphology. *J. Appl. Crystallogr.* **2015**, 48 (1), 189–194.
- (21) Coughlan, C.; Ibáñez, M.; Dobrozhan, O.; Singh, A.; Cabot, A.; Ryan, K. M. Compound Copper Chalcogenide Nanocrystals. *Chem. Rev.* 2017, 117 (9), 5865–6109.
- (22) Jain, A.; Ong, S. P.; Hautier, G.; Chen, W.; Richards, W. D.; Dacek, S.; Cholia, S.; Gunter, D.; Skinner, D.; Ceder, G.; Persson, K. A. Commentary: The Materials Project: A Materials Genome Approach to Accelerating Materials Innovation. *APL Mater.* **2013**, *1* (1), 011002.
- (23) Jain, A.; Hautier, G.; Ong, S. P.; Moore, C. J.; Fischer, C. C.; Persson, K. A.; Ceder, G. Formation Enthalpies by Mixing GGA and GGA + U Calculations. *Phys. Rev. B* **2011**, *045115*, 1–10.
- (24) Agocs, D. Hot Injection Synthesis and Characterization of Copper Antimony Selenide Non-Canonical Nanomaterials toward Earth-Abundant Renewable Energy Conversion; Colorado State University: 2018.
- (25) Yarema, O.; Bozyigit, D.; Rousseau, I.; Nowack, L.; Yarema, M.; Heiss, W.; Wood, V. Highly Luminescent, Size- and Shape-Tunable Copper Indium Selenide Based Colloidal Nanocrystals. *Chem. Mater.* **2013**, 25 (18), 3753–3757.